DOI: https://doi.org/10.68732/44bb7e987978519c

ISBN: 978-9989-2053-6-1

Optimal Stoping Limits, Stability, and Dip Pillars for Seismicity: SA Gold Mine

R. T. Masethe; O. Vetman & T. Sibiya
College of Agriculture, Engineering and Science, University of KwaZulu-Natal, Durban, South Africa
masetheR@ukzn.ac.za
0000-0002-4420-7885

Abstract

This study integrates two critical geotechnical investigations conducted at a shallow gold mine in South Africa, focusing on optimal stoping limits, ground stability, and the effectiveness of stabilizing dip pillars within broader seismicity management strategies. The first component evaluates the optimal stoping limit for the 202 N S1 Raise Line to minimise abutment stress on the underlying 202 N Returned Air Way (RAW). Geological complexities, including major faults dipping at 65° and 85° south, minor discontinuities, and an over-excavated section measuring 4.4–4.8 m, necessitated a rigorous assessment of ground stability. Numerical modelling using IMS Vantage tested stoping spans of 5 m, 10 m, and 15 m to determine their impact on the Rock Condition Factor (RCF). Although a 15 m span produced the most favourable stability conditions, it was economically unviable. The 10 m stoping limit emerged as the optimal compromise, with localised instability addressed through a combination of resin-grouted bolts, mesh, lacing, and shotcrete to mitigate Fall of Ground (FOG) risks. The second component investigates the performance of 15 m stabilizing dip pillars, introduced in 2020 to manage seismicity, which nevertheless continued to escalate by 2023 with increasing seismic events of large magnitude ($M_L \geq 2.0$). These seismic events produced damaging rockbursts that threatened safety and disrupted production. Analysis revealed limitations in the dip pillar design and inconsistent adherence to seismicity management principles, including bracket pillar placement and lead-lag formation. Comparative assessments of Average Pillar Stress (APS), face stress, closure rates, and seismic response between compliant and non-compliant mining areas highlighted the need for improved pillar configurations. Overall, the research underscores the importance of optimised stoping spans, robust support strategies, and strict compliance with seismicity management principles to enhance ground stability, reduce seismic hazards, and sustain safe, efficient production at a shallow gold mine.

Keywords

Average Pillar Stress, Moment Tensor, Field stresses, Rock Condition Factor.

1 Introduction

1.1 Background of the study area

The geology of the Witwatersrand Basin has been widely studied (Beach & Smith, 2007; Fletcher, 2009; Viljoen, 2009; Dankert & Hein, 2010). The basin formed between about 3.07 and 2.71 billion years ago as a result of tectonic interactions between the Zimbabwe and Kaapvaal cratons (Armstrong et al., 1991; Robb & Meyer, 1995). These interactions created a foreland basin in which several stratigraphic units were deposited above a granite–greenstone basement. The earliest deposits were the volcano-sedimentary rocks of the Dominion Group, which were later overlain by the Witwatersrand Supergroup. This supergroup is divided into the lower West Rand Group (WRG), composed mainly of quartzites and ferruginous shales deposited in shallow marine environments, and the upper Central Rand Group (CRG), which is dominated by quartzites and gold-bearing conglomerates (McCarthy, 2006; Dankert & Hein, 2010). Sedimentation began in shallow marine conditions and gradually shifted to more continental environments as the basin filled and regressed (Tucker et al., 2016). The basin, located in South Africa, developed over roughly 360 million years and is recognised as the world's largest gold-producing basin (see Fig. 1)

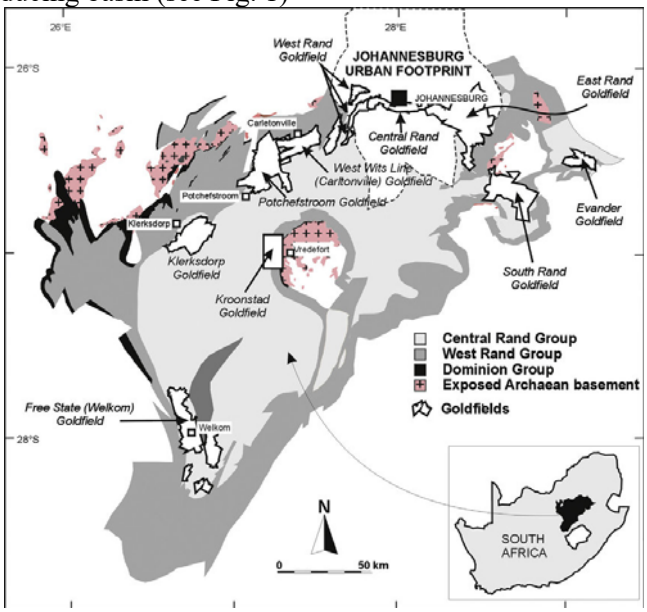


Fig. 1 A diagrammatic representation of the study area from the Witwatersrand Basin (modified from Dankert and Hein, 2010).

The West Rand Group forms the lower portion of the Witwatersrand Supergroup and averages about 4,500 m in thickness (Tainton & Meyer, 1990). It is mainly composed of quartzites and shales in roughly equal proportions, representing shallow-marine shelf sand bodies and finer sediment deposits (Pretorius, 1979; Eriksson et al., 1979; Beukes & Nelson, 1995). Magnetite-bearing shale layers within the group serve as important magnetic markers for deep basin exploration (Tucker et al., 2016). The WRG developed in response to mechanical subsidence within a pull-apart basin formed under trans-tensional rifting conditions (Maynard & Klein, 1995) and is subdivided into the Hospital Hill, Government, and Jeppestown subgroups (Johnson et al., 2006). These subgroups record varying depositional settings, ranging from shallow-marine quartzites and outer-shelf shales in the Hospital Hill Subgroup to lithologically diverse sequences in the Government Subgroup that include conglomerates, iron formations, and diamictites. The Jeppestown Subgroup contains a range of rock types and records a transgressive sequence marked by upward-fining quartzites that grade into shales and iron formations.

The Central Rand Group overlies the West Rand Group and differs significantly in composition and depositional environment. It contains a higher proportion of quartzites and conglomerates, with a quartzite-to-shale ratio of approximately 12:6 (Pretorius, 1976), and the quartzites are typically feldspar-poor (Law et al., 1990). This group represents the upper part of the Witwatersrand Supergroup and hosts most of the basin's gold deposits, particularly within conglomeratic reef horizons (Sanders et al., 1994). The CRG is subdivided into the Johannesburg and Turffontein subgroups. The Johannesburg Subgroup consists mainly of quartzites deposited in fluvial braid-plain environments, while the Turffontein Subgroup represents the final stage of sedimentation in the basin, characterised by prograding braid-plain deposits and conglomeratic units associated with placer gold mineralisation, such as the Kimberley Reef (Johnson et al., 2006; McCarthy et al., 1990). The

geological history of the basin was later modified by major events including tectonic deformation, the Vredefort meteorite impact, and the emplacement of the Bushveld Complex, all of which contributed to metamorphism and partial remobilisation of gold mineralisation (SACS, 1980; Tucker et al., 2016).

1.2 Locality of the area of study, mining methods, and the effects of geological structures

The study area is located within the Witwatersrand Basin in Gauteng, approximately 30–40 km west of Johannesburg. The mining operations occur along the northern margin of the basin and target the South Reef, which forms part of the Central Rand Goldfields. Stratigraphically, the South Reef occurs about 80 m above the Main Reef Leader and is characterised by several pebble bands associated with gold mineralisation (Viljoen et al., 2016; Viljoen, 2009). The reef has historically been regarded as one of the major gold-producing horizons in the Central Rand and is considered the stratigraphic equivalent of the Nigel Reef in the East Rand Goldfields (Viljoen et al., 2016). Lithologically, the South Reef typically ranges from about 1 to 1.5 m in thickness and consists of a basal pebble lag containing a gold-rich bitumen seam overlain by conglomerates interbedded with quartzites (Johnson et al., 2006).

Mining operations in the study area exploit this reef at intermediate depths ranging between approximately 1,650 and 2,000 m below surface, where the orebody occurs as a thin, carbonaceous, and friable seam that is economically viable for extraction (Stacey, 1989). The reef is gently inclined at about 10° towards the southeast and lies approximately 900 m below the Kimberley Reef. Although the South Reef is relatively thin, in some areas measuring only a few centimetres in thickness, it contains a high proportion of free gold, with mineralisation reaching roughly 70%, making it highly attractive for underground mining despite the associated technical challenges (Grave, 2009). Structurally, the orebody is bounded and segmented by several major geological features, including the Roodepoort Fault, the Witpoortjie Horst, and local fault systems such as the Saxon Faults, which divide the reef into large structural blocks and influence ground stability during mining (Stacey, 1989).

Deep-level gold mining within the Witwatersrand Basin occurs at depths commonly exceeding 1,500 m below surface, where high in-situ stresses significantly influence excavation stability. Under these conditions, mining-induced seismicity and rock mass deformation represent major geotechnical challenges. Stress levels in such environments can exceed 100 MPa, creating conditions that increase the likelihood of seismic events, rockbursts, and hanging-wall instability. Consequently, the design of underground excavations requires careful evaluation of stope geometry, extraction sequences, and support systems to ensure safe and efficient operations in South African gold mines

1.2.1 Mining methods

Mining methods in deep-level underground operations are designed to maximise ore extraction while maintaining ground stability and minimising geotechnical hazards. In South African gold mines, particularly those exploiting the Ventersdorp Contact Reef (VCR), Sequential Grid Mining (SGM) has become an important mining strategy for managing the high-stress conditions associated with deep mining. SGM was developed at Kusasalethu Mine in the late 1980s as an alternative to longwall and scattered mining methods, which were associated with significant stress concentrations and frequent rockburst occurrences (Handley et al., 2000). The method involves the systematic extraction of ore through a grid of raises and crosscuts, typically spaced approximately 200 m apart, creating mining panels supported by dip stabilising pillars (see Fig. 2). These pillars, commonly around 30 m wide, provide regional support and regulate stress redistribution within the rock mass, thereby controlling the Energy Release Rate (ERR) and improving ground stability during mining (Handley et al., 2000). This design enables extraction efficiencies of approximately 85%, although pillar size and spacing are adjusted according to mining depth and stress conditions.

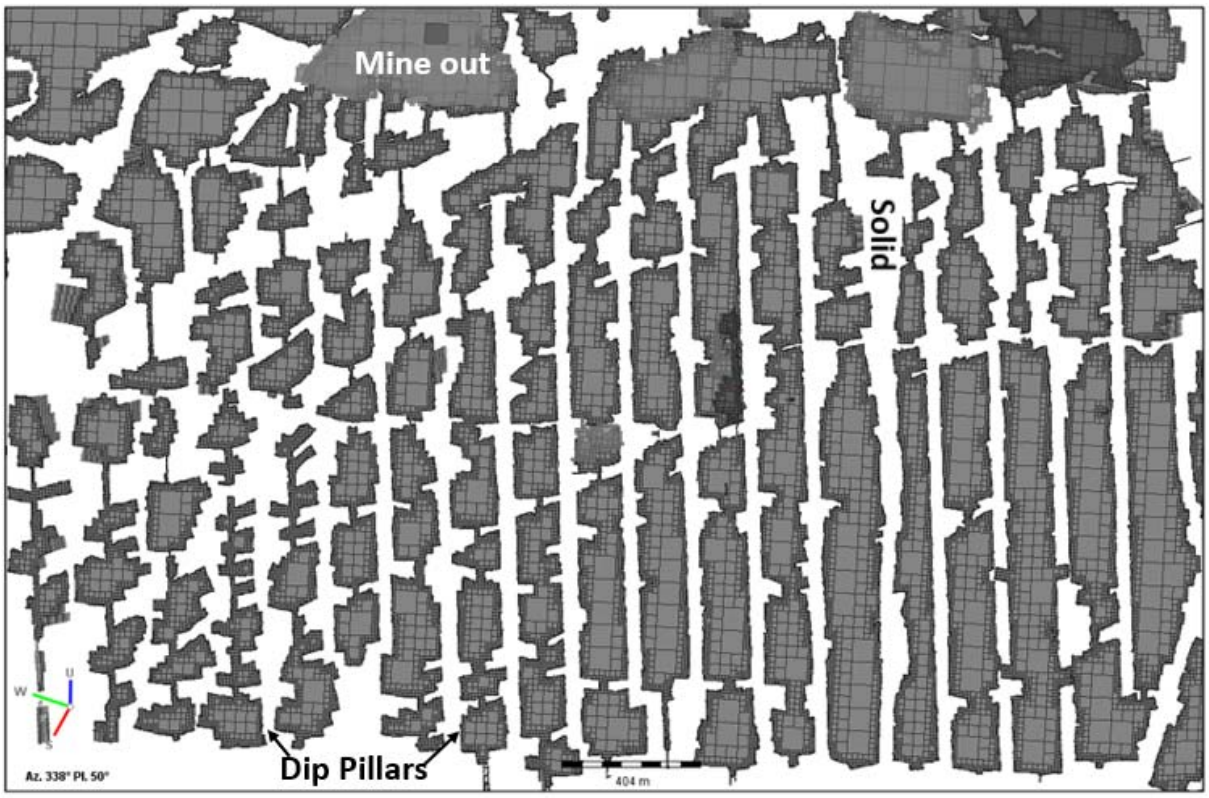


Fig. 2 Sequential grid mining layout (SGM) in the Witwatersrand basin.

The SGM layout typically maintains a V-shaped mining configuration down-dip, which promotes more uniform stress distribution as mining progresses (Jooste & Malan, 2015). This configuration also allows geological structures to be bracketed within stabilising pillars, which reduces the risk of seismic events associated with structural reactivation. Additional advantages of the method include reduced off-reef development and improved selectivity in areas where ore grades are erratic or geological conditions are complex (Jooste & Malan, 2015). However, the strict sequencing requirements of SGM can limit production flexibility and may result in slower production rates and higher upfront development costs. To address these challenges, modified approaches such as multi-raise mining methods have been introduced while retaining the key safety and stability benefits of the original SGM concept.

1.2.2 The effects of geological structures

The performance and safety of underground mining methods are strongly influenced by the presence of geological structures such as faults, joints, and dykes. These structures significantly affect rock mass behaviour, stress redistribution, and the stability of underground excavations. Faults are particularly critical in deep mining environments because they can be reactivated by mining-induced stress changes. When a slip occurs along a pre-existing fault plane between the hanging wall and footwall, sudden dynamic loading may be generated, which can trigger seismic events or rockbursts that threaten worker safety and disrupt production activities (Li et al., 2008; Chen et al., 2012). Faults can also displace the ore body, complicating mining layouts and reducing the stability of surrounding rock masses (Zhou et al., 2023). In many cases, sudden slips along faults during mining can cause large-scale instability within the surrounding rock mass, resulting in dynamic failures such as seismic events or rockbursts (Zhou et al., 2023). As a result, fault zones are considered critical features in mine planning and must be carefully incorporated into mining layouts and support designs.

Joints and other discontinuities also play a major role in the mechanical behaviour of rock masses in underground mining environments. These planes of weakness reduce the shear strength of rock masses and influence the distribution of stresses around excavations, which can increase deformation and the likelihood of failure (Chen et al., 2023). The orientation and continuity of joints are particularly important, as certain joint angles relative to the stress field, commonly between 30° and 45°,can significantly reduce rock mass strength and increase displacement around underground openings (Liu et al., 2021). Depending on their distribution and orientation, joints may lead to different failure

mechanisms, including rockbursts, block rotation, or sliding failures (Qie et al., 2023). Consequently, accurate joint mapping and probabilistic rock mass analyses are essential for predicting rockfall hazards and designing appropriate support systems (Zhou et al., 2023).

Dykes represent another important geological feature that influences mining operations and rock mass behaviour. These igneous intrusions typically form along pre-existing fractures such as faults and joints and often possess mechanical properties that differ significantly from those of the surrounding host rock (Bell, 1983; Keneti & Sainsbury, 2020). The contrast in stiffness and strength between dyke material and surrounding rock can result in stress concentration zones that increase the likelihood of sudden rock failure. Studies have shown that the risk of strain bursts is often higher near dyke contacts due to these stress concentrations (Duan et al., 2022). In the South African mining industry, dolerite dykes are particularly common and are known for their high strength and brittle behaviour under tectonic stress conditions (Wagner & Schumann, 1991; Demenkov & Basalaeva, 2025). Their presence can therefore significantly influence mine design, support requirements, and extraction sequences.

In underground mining operations, the stope and access layout are two critical components that must be optimised during the design phase. These elements cannot be considered independently because ore extracted from stopes must be transported to the surface through the access network (Hou et al., 2019). Optimal stoping limits, therefore, play a fundamental role in balancing ore recovery with ground stability (Jager & Ryder, 1999). The design of underground excavations must consider several geotechnical parameters, including rock strength, in-situ stress conditions, and the geometry of the orebody (Jager & Ryder, 1999). Ground stability analysis is essential for evaluating rock mass behaviour under stress and identifying potential hazards such as subsidence, rockfall, and seismic instability (Ryder & Jager, 2002). Appropriate ground support systems must then be designed based on these analyses to mitigate risks and maintain excavation stability, while continuous monitoring during mining operations allows for adjustments as conditions evolve (Potvin et al., 2019).
To mitigate seismic risk and ensure geotechnical stability in deep-level mining environments, dip pillars with a width of approximately 75 m are frequently integrated into the mining layout. These structures act as regional support elements, separating mining panels (approximately 175 m in span) to effectively regulate the redistribution of mining-induced stresses (Jager & Ryder, 1999). By limiting the extent of extraction and stabilising geological structures such as faults and joints, dip and bracket pillars reduce the likelihood of large seismic events triggered by mining activities. However, as mining progresses deeper and extraction ratios increase, the long-term effectiveness of these pillars requires ongoing evaluation to ensure that they continue to provide adequate support and control seismicity. Numerical modelling has become an essential tool for evaluating underground excavation stability and optimising stope design. These modelling techniques allow geotechnical engineers to predict deformation patterns, assess stress redistribution, and estimate support loads using integrated geological and geotechnical data (Coulthard, 1999). In addition, numerical models serve as investigative tools for assessing uncertainties and evaluating potential risks associated with underground mining (Fels & Elmo, 2022). Within these analyses, parameters such as the Rock Condition Factor (RCF) are used to quantify rock mass quality and its response to mining-induced stresses, thereby guiding the design of reinforcement systems and determining appropriate stope dimensions (Hoek & Brown, 1980). Through such approaches, optimal stoping limits, stability conditions, and dip pillar configurations can be established to minimise seismic hazards while maintaining productive mining operations in South African gold mines.

2 Optimal Stoping Limits

The 202 N S1 Raise represents a relatively short excavation, approximately 70 m in length, but it is situated within a geologically complex and structurally constrained environment. The raise is intersected and influenced by several significant geological discontinuities, of which two major fault structures play a dominant role in controlling both the mining layout and the achievable extraction span. The first structure is a fault dipping at 65° to the south, with an estimated displacement of ±31 m. This fault effectively separates the N1 RAWand N1 S1 Raise Lines, acting as a key structural boundary within the mining area. The second fault, positioned toward the upper extent of the raise line, is steeper, dipping at approximately 85°, with a larger displacement of ±68 m. Importantly, the

202 N S1 Raise the focus of this study is located on the structurally weaker side of this latter fault, which has direct implications for stability and stoping design.

As illustrated in Fig.3, these two faults define the structural framework within which the raise exists. The highlighted zones show their spatial relationship to the raise line and surrounding excavations. However, several critical aspects influencing the case study are not explicitly visible in the image. Most notably, the figure does not depict the presence of a middling of approximately 14 m between the base of the raise and the N1 RAW. This middling introduces a significant design concern, as abutment stresses generated during stoping operations at the base of the raise are likely to transfer upward and accumulate above the N1 RAW. This stress interaction is a key factor in determining safe and optimal stoping limits.

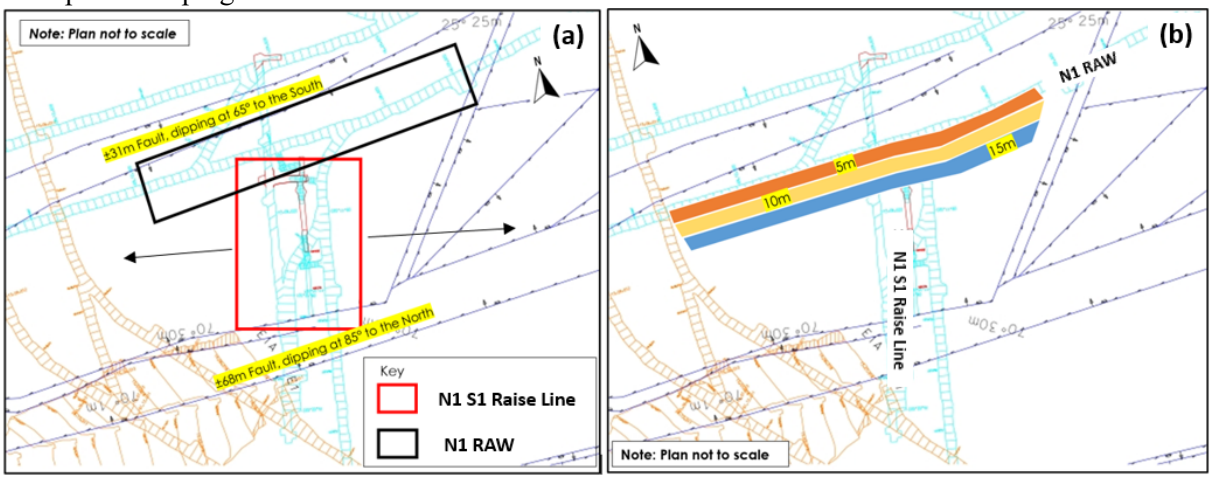


Fig. 3 (a) The mining Plan illustrates the N1 RAW, N1 S1Raise line, and two major faults, and the arrows indicate mining direction. (b) Plan showing the modelled scenarios (5, 10, 15 m) away from the N1 RAW.

Additionally, the historical mining practices that have affected the current excavation geometry are not shown. During early development, the upper section of the raise was mined off-reef, leaving the footwall in place due to poor mining practices. Subsequent footwall ripping was later conducted to expose the orebody. This resulted in an oversized excavation, with a maximum height reaching approximately ±4.8 m. Figure 3(b) does not capture the overbreak or the irregular excavation profile, both of which are critical to understanding the current stability conditions.

The underground assessment focused on evaluating the physical condition of the raise line and its associated infrastructure. The N1 RAW was equipped with primary support consisting of shepherd's crook tenders; however, no secondary support had been installed. The crosscut (X/cut) was supported using end-anchored Kat-bars in conjunction with welded mesh, and no adverse ground conditions were observed in this area. Overall, ground conditions along the raise line were generally satisfactory, with only minor localised concerns observed in both the N1 RAW and the raise line. Despite these largely stable conditions, the reduced middling thickness between the raise base and the N1 RAW introduces a potential risk of progressive abutment stress transfer.

To assess and mitigate this risk, IMS Vantage numerical modelling software was utilised. The primary objective of the analysis was to determine the optimal stoping limit at the base of the raise line. This was achieved by evaluating variations in the Rock Condition Factor (RCF) across three proposed stoping scenarios, located 5 m, 10 m, and 15 m from the RAW, as defined in the mining plan (See Fig. 4b).

The Rock Condition Factor (RCF), developed by Wiseman (1979) of the Chamber of Mines, South Africa, is a practical measure used to assess tunnel stability by relating induced stress at the excavation boundary to the strength of the rock mass. It is expressed as (see Eq. 1).

$$RCF = \frac{3\sigma_1 - \sigma_3}{F\sigma_c} \qquad (1)$$

where σ_1 and σ_3 represent the maximum and minimum field stress components in the plane of the excavation cross-section, σ_c is the uniaxial compressive strength of the intact rock, and F represents a reduction parameter that accounts for the weakening effect of geological discontinuities on rock mass strength. In competent, relatively intact rock, F is close to 1, whereas in highly jointed or bedded rock masseswith discontinuities spaced less than about 0.1 m, F is typically reduced to approximately 0.5. For larger excavations (e.g., 6 × 6 m compared to standard 3 × 3 m tunnels), F is further reduced by about 20% to reflect the additional weakening associated with excavation size. This simplified approach, which integrates both analytical and numerical considerations, provides a practical and efficient design tool requiring limited input parameters (Jager & Ryder, 1999).

At the mine, the Rock Condition Factor (RCF) is used as a primary indicator for assessing ground conditions and guiding support design. RCF values below 0.7 indicate stable ground requiring minimal support, values between 0.7 and 1.4 represent intermediate conditions needing moderate support, and values equal to or greater than 1.4 indicate unstable ground that requires specialised support systems. The influence of jointing is directly incorporated through the factor F, where F = 1 corresponds to intact rock and F = 0.5 represents highly jointed rock masses

The Rock Condition Factor was applied to evaluate model sensitivity and determine optimal stoping limits of 5 m, 10 m, and 15 m. The aim was to improve production efficiency while minimizing stress-induced damage to the rock at the working (RAW) face through optimized layout design and appropriate support systems. These simulations provide insight into the relationships among mining geometry, stress distribution, and ground support performance, thereby informing safer and more productive underground excavation strategies. For the N1 RAW, Fig. 4(a) shows that at a 5 m stoping limit (measured from the bottom of the N1 S1 raise line), RCF values exceed 1.12, corresponding to average ground conditions as defined by Wiseman (1979). This suggests that mining up to 5 m would generally yield average stability along the full strike span of over 150 m, with additional support required throughout the RAW.

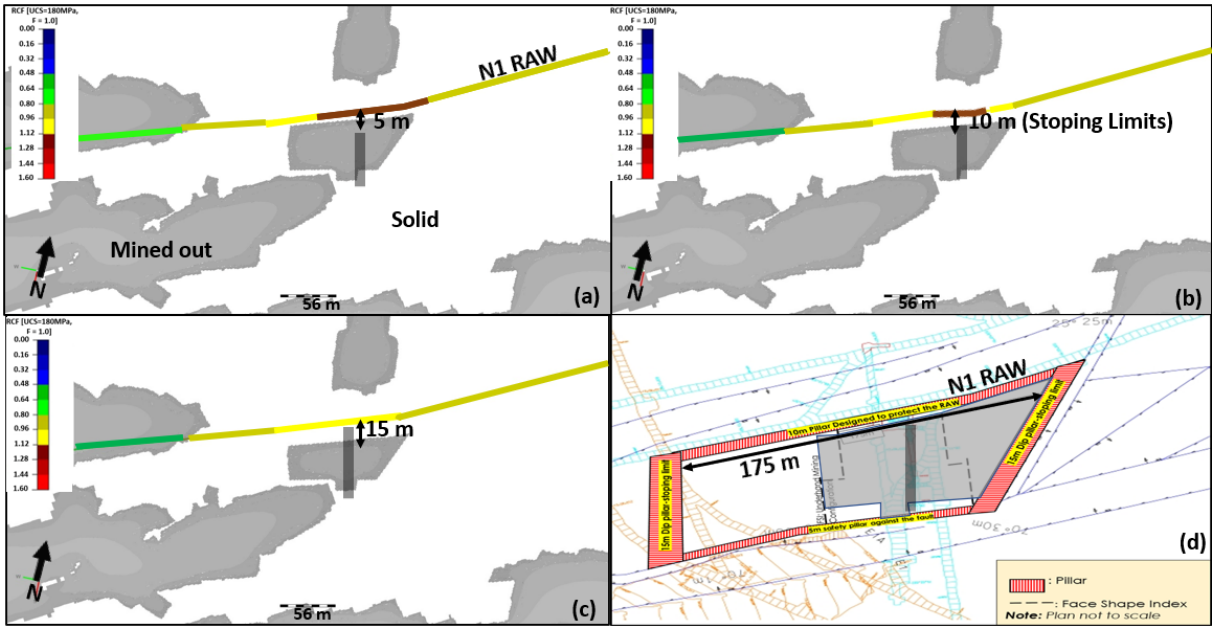


Fig. 4 (a) Rock Condition Factor (RCF) of 5 m stoping limit, (b) RCF of 10 m Stoping limit, (c) RCF of 15 m Stoping limit, and (d) 202 N S1 Raise Line overall mining layout.

At increased stoping limits, ground conditions show progressive improvement. Fig. 4(b) indicates that at a 10 m stoping limit, RCF values remain above 1.12, still reflecting average conditions, but the extent of concern is reduced compared to the 5 m case. Instability is expected to be localized primarily around the intersection of the N1 RAW and the N1 S1 crosscut, suggesting the benefit of a wider pillar. However, secondary support would still be required in this zone. Fig. 4(c) further demonstrates that at a 15 m stoping limit, RCF values range between 0.96 and 1.12, indicating improved and more stable average ground conditions relative to the other scenarios. This reflects a notable enhancement in stability, with the 15 m pillar showing strong potential to mitigate instability in the N1 RAW and reduce the need for extensive support. However, further analysis may still be warranted.

Considering the relatively short length of the N1 S1 Raise Line (approximately 70 m), a 5 m stoping limit is not recommended due to the highly unstable ground conditions in the N1 RAW, which would necessitate technically demanding and costly specialized support systems such as yielding props, cable anchors in the tunnels, or backfilling in the operating stopes. Conversely, a 15 m stoping limit is also unsuitable; although the rock mass under this scenario demonstrates good stability with only minimal reinforcement required (e.g., rockbolts or mesh), the increased mining span reduces the extractable area, thereby limiting ore recovery and negatively affecting production efficiency and profitability. A 10 m stoping limit between the Raise Line and the RAW is therefore recommended, as it achieves an optimal balance between ore extraction, rock stability, and cost-effective support requirements, maximizing the available mining block while minimizing the risk of stress-induced fracturing or overstoping. As illustrated in Figure 4(d), the overall mining layout shows that the blank spaces represent remaining extractable ore panels, underscoring the economic advantage of adopting the 10 m limit to ensure both safety and sustainable production.

3 Stability, Dip Pillar Layout

The mine continues to experience persistently high seismic activity despite the introduction of 15 m-wide stabilizing dip pillars in April 2020, posing ongoing safety and operational challenges. By 2023, mining-induced seismic events ($M_L \geq 2.0$) had increased, elevating the risk of rockbursts that threaten worker safety, damage infrastructure, and disrupt production. This trend indicates that the current pillar design may not be effectively mitigating seismic hazards, highlighting the need to reassess the use of 15 m dip pillars. The existing conceptual framework, based on a grid of dip and bracket pillars, aims to control Energy Release Rates (ERR), maintain Average Pillar Stress (APS) within safe limits (~ 27–30 MPa), and incorporate geological structures such as dykes through planned mining sequences; however, its effectiveness under current conditions remains uncertain.

The Sequential Grid Mining model was originally developed to enable safe, high extraction in deep-level mining while maintaining ERR below 20 MJ/m², but its implementation, along with seismic management strategies such as lead-lag configurations and bracket pillars, has not been fully evaluated at this mine. In addition, limited data on time-dependent pillar (creep) behaviour and seismic indicators, such as pillar strain, restricts a comprehensive understanding of the problem. Time-dependent behaviour involves gradual deformation, delayed fracturing, and stress redistribution within pillars under sustained loads, often exacerbated by the growth of fractures over time. This process can lead to scaling, effectively reducing pillar width, increasing stress concentrations, and ultimately raising the likelihood of pillar failure, thereby contributing to the observed seismicity.

This section aims to evaluate the effectiveness of the 15 m-wide stabilizing dip pillars implemented at this Shaft and assess their compliance with seismicity management principles in mitigating seismic activity. It examines their performance in the context of the continued increase in seismic events (ML ≥ 2.0) observed by 2023, while also assessing alignment with key practices such as lead-lag configurations and bracket pillars. The study further compares closure rates, face stress, Average Pillar Strength (APS), and seismic response between compliant and non-compliant areas to understand how adherence influences seismic risk. It also highlights limitations in the current pillar design, particularly the lack of data on time-dependent pillar behaviour, and proposes improvements to enhance safety and operational efficiency. The following input parameters were used in the numerical model: Young's Modulus (E) - 70GPa, Poisson's Ratio (v) - 0.2, Depth - 1793m, Vertical stress (σ_{zz}) – 0.02750 MPa/m, Stress on x-direction (σ_{xx}) - 0.013750 MPa/m, Stress on y-direction (σ_{yy}) – 0.013750 MPa/m, Static friction angle – 25^o, Dynamic friction angle –20 °, Cohesion – 0 MPa.

Figures 5(a) and (b) present the Average Pillar Stress (APS) model for raise line S (polygons 1D–5D) and raise line N (polygons 1B and 2B). The results show that, irrespective of compliance with pillar sizes and stoping limits, one pillar in raise line S (polygon 4D) is subjected to elevated stress levels of 350–375 MPa, likely due to scaling or time-dependent (age-related) behaviour. In contrast, another pillar within the same polygon experiences lower stresses of 275–300 MPa, with this variation attributed to excessive mining spans, underscoring the importance of adhering to design limits in controlling APS. Similarly, isolated pillars in polygons 2D and 1D of raise line S exhibit elevated stress levels (325–350 MPa), as they are more susceptible to overloading due to uneven stress distribution when mining spans are exceeded. This observation supports findings by Jager and Ryder (1999; 2002) that poor design and excessive spans increase the likelihood of instability and pillar

failure. Notably, one 15 m-wide dip pillar in polygon 4D performs adequately, with a stress of 275 MPa, below the maximum allowable limit of 325 MPa.

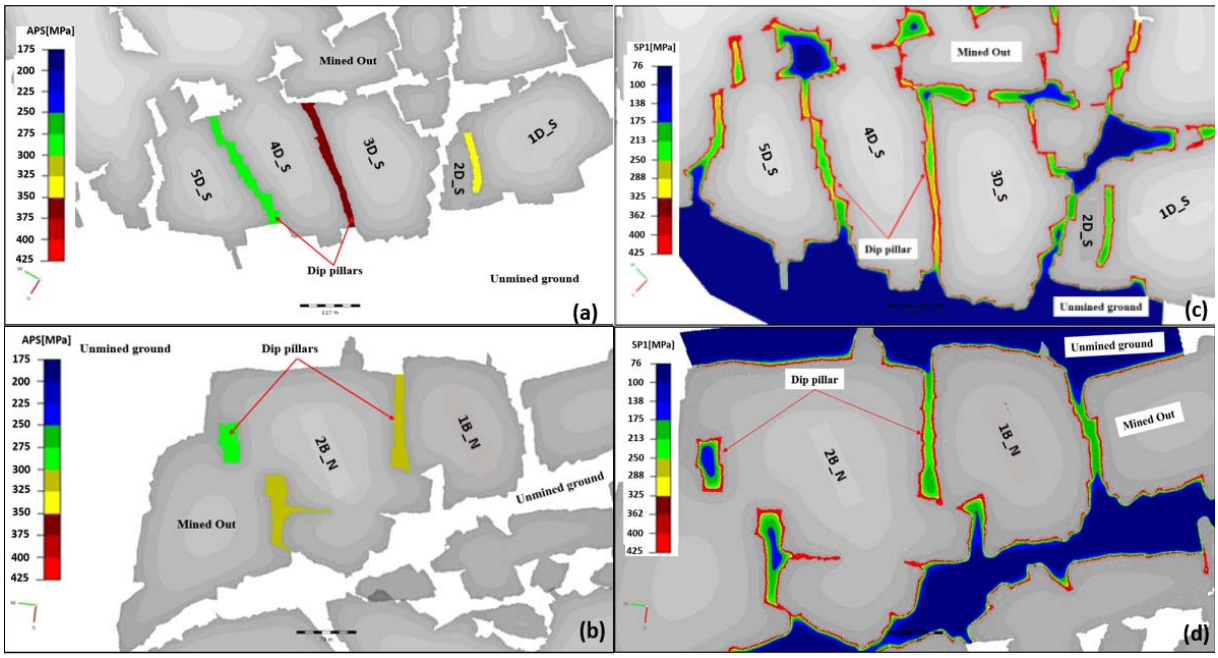


Fig. 5(a) Average Pillar Stress (APS) model for the raise line S in polygon 1D-5D (b) APS model for the raise line N for polygons1B and 2B. (c) Face Stress Model (FSM) for the raise line S in polygon 1D-5D and (d) FSM in B and 2B.

A similar trend is observed in raise line N (polygon 2B), where pillars experience elevated stresses ranging from 275 to 325 MPa, as shown in the APS model. These conditions are attributed to poor compliance with lead-lag sequencing, the presence of isolated pillars, and excessive mining spans, all of which contribute to uneven stress distribution and increased seismic risk. Isolated pillars, in particular, are more vulnerable to overloading as they bear disproportionate loads in expanding mining environments, leading to instability. However, as in raise line S, one dip pillar in polygon 2B performs well, maintaining stress levels below 300 MPa. Overall, the findings indicate that practices such as partial or complete mining of stabilizing dip pillars, leaving remnant or undersized pillars, and inadequate spacing contribute to elevated stress concentrations, increasing the risk of pillar failure and associated seismic activity.

Face stress represents the maximum principal stress acting normal to the advancing mining face and is a critical factor influencing rock fracturing, rockbursts, and overall working conditions. Elevated face stresses, particularly in high-extraction environments, are widely recognized as a major contributor to increased seismic hazard potential. Fig. 5(c) and (d) demonstrate the relationship between face stress, mining span, and dip pillar positioning, showing that as mining spans increase and panels advance toward dip pillars, stress levels rise in both raise lines S and N. The model results indicate that face stresses exceed the permissible threshold of 300 MPa, primarily due to excessive mining spans, non-compliance with dip pillar design and spacing, and panel holing near raise lines.
These elevated stresses, especially those associated with panel holing and poor adherence to seismicity management principles, are linked to an increased likelihood of larger seismic events, reinforcing findings from previous studies that emphasize the importance of pillar stability in controlling rock mass failure (Jager and Ryder, 1999). The results further show that inadequate dip pillar spacing, remnant and isolated pillars, and uncontrolled panel advancement contribute to stress concentrations beyond safe limits, leading to instability and heightened seismic activity. Effective face stress management can therefore be achieved through controlled panel advancement, optimized pillar design, and strict adherence to dip pillar spacing and mining span guidelines, all of which are essential for mitigating seismic risks and ensuring long-term excavation stability.

4 Closure and Numerical Modelling

The closure model provides insight into how elevated stress levels from overlying strata cause convergence between the hanging wall and footwall in underground mines. Fig. 6 shows that 15 m-

wide stabilizing dip pillars can effectively reduce closure when properly implemented, as seen in polygons 5D and 4D of raise line S. However, excessive closure of 0.30–0.35 m is observed in polygons 1D_S and 3D_S, significantly reducing centre gully height and creating unsafe working conditions, particularly for post-mining activities such as infrastructure reclamation. These poor conditions are linked to non-compliance with dip pillar design, excessive mining spans, and older workings where dip pillars were not installed.

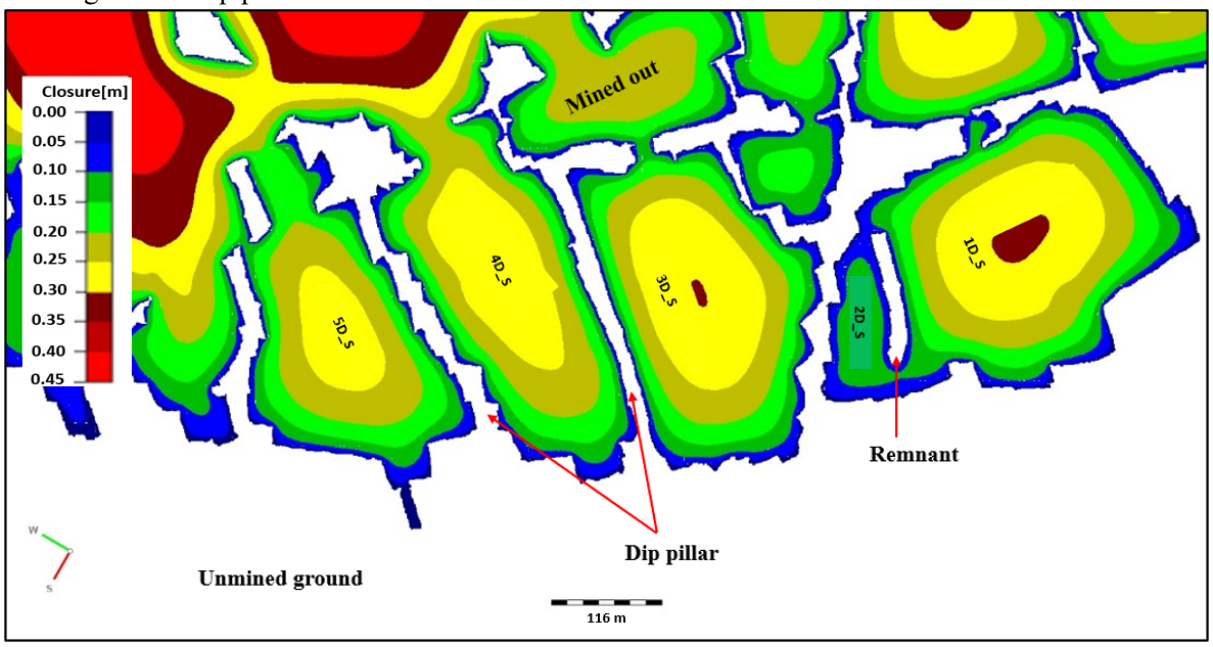


Fig. 6 Closure model for the raise line S for polygons (e.g.,5D, 4D, 3D, 2D, and 1D).

Closure monitoring through loggers, manual measurements, and calculations using rock properties remains essential for assessing these risks. Overall, the results highlight that proper adherence to dip pillar design and controlled mining spans is critical in reducing closure, maintaining excavation stability, and ensuring safer underground working conditions.

5 Conclusion

Optimum Stoping Width: Numerical modelling confirms that a 10 m stoping limit provides the best balance between ground stability and production efficiency. While a 5 m limit results in widespread unstable conditions requiring costly support, and a 15 m limit improves stability but reduces ore recovery, the 10 m span effectively localises instability to the RAW crosscut intersection and minimises risks such as stress-induced fracturing and overstoping. To manage these localised high-stress zones, a combination of active (grouted rock bolts) and passive (mesh and shotcrete) support is recommended to enhance rock mass integrity, reduce fall-of-ground risks, and ensure long-term excavation stability.

Seismicity and Pillar Design: The study further shows that the effectiveness of 15 m-wide stabilizing dip pillars is highly dependent on strict compliance with design and seismicity management principles. Where correctly implemented, pillars reduced stress, closure, and seismic risk, improving safety and productivity; however, poor adherence, such as incorrect support spacing, excessive mining spans, and panel holing, led to elevated stress levels, instability, and increased seismic events, including production disruptions. Overall, maintaining proper pillar design, spacing, and mining practices is essential to control seismicity, reduce closure, and ensure safe, sustainable mining operations.

References

Armstrong RA, Compston W, Retief EA, Williams IS, Welke HJ (1991) Zircon ion microprobe studies bearing on the age and evolution of the Witwatersrand Basin. Precambrian Research 53(3–4): 243–266. https://doi.org/10.1016/0301-9268(91)90074-K.

Beach DA, Smith ND (2007) Geological evolution of the Witwatersrand Basin and its sedimentary environments. Journal of African Earth Sciences 48(2): 123–145.

Bell FG (1983) Engineering properties of rocks. Butterworths, London.

Beukes NJ, Nelson DR (1995) Depositional environments of the West Rand Group. Journal of African Earth Sciences 21(3): 345–360.

Chen Z, Li X, He M (2012) Rockburst mechanisms and prediction in deep mining. Rock Mechanics and Rock Engineering 45(6): 1023–1035.

Coulthard MA (1999) Numerical modelling in geomechanics. Report Series. Institution, Location.

Dankert BT, Hein KAA (2010) Geology and gold mineralisation of the Witwatersrand Basin. Ore Geology Reviews 36(1–3): 1–15.

Demenkov PS, Basalaeva EM (2025) Mechanical behaviour of dolerite under stress conditions. Rock Mechanics and Rock Engineering 58(1): 45–60.

Duan K, Li X, Zhou J (2022) Strain burst mechanisms near geological discontinuities. Rock Mechanics and Rock Engineering 55(3): 1501–1515.

Eriksson KA, Truswell JF, Eriksson PG (1979) Sedimentology of the Witwatersrand Basin. Precambrian Research 9(1–2): 1–27.

Fels L, Elmo D (2022). Numerical modelling for underground excavation design. International Journal of Rock Mechanics and Mining Sciences 152: 105050. https://doi.org/10.1016/j.ijrmms.2022.105050.

Fletcher CJN (2009) Sedimentology and stratigraphy of the Witwatersrand Supergroup. South African Journal of Geology 112(3): 201–220.

Grave EJ (2009) Gold mineralisation characteristics of the South Reef. Dissertation at the University of the Witwatersrand.

Handley MF, Stacey TR, Malan DF (2000) Sequential grid mining in deep-level gold mines. Journal of the South African Institute of Mining and Metallurgy 100(1): 25–32.

Hoek E, Brown ET (1980) Empirical strength criterion for rock masses. Journal of the Geotechnical Engineering Division 106(9): 1013–1035.

Hou Z, Xie H, Zhang R (2019) Optimization of underground mining layouts. International Journal of Mining Science and Technology 29(3): 345–352. https://doi.org/10.1016/j.ijmst.2019.03.003.

Jager AJ, Ryder JA (1999) A Handbook on Rock Engineering Practice for Tabular Hard Rock Mines. Safety in Mines Research Advisory Committee, Johannesburg.

Johnson MR, Anhaeusser CR, Thomas RJ (2006) The Geology of South Africa. Geological Society of South Africa, Johannesburg.

Jooste Y, Malan DF (2015) The application of sequential grid mining in South African gold mines. Journal of the Southern African Institute of Mining and Metallurgy 115(2): 123–132.

Keneti A, Sainsbury BA (2020) The influence of dykes on rock mass behaviour in underground mining. International Journal of Rock Mechanics and Mining Sciences 128: 104267 https://doi.org/10.1016/j.ijrmms.2020.104267.

Law JD, Phillips GN, Groves DI (1990) Geochemistry of Witwatersrand quartzites. Journal of Geochemical Exploration 36(1–3): 123–145.

Li X, Chen Z, Zhou J (2008) Dynamic loading and seismic response in underground excavations. International Journal of Rock Mechanics and Mining Sciences 45(6): 1003–1012.

Liu Q, Jiang Q, Feng X (2021) Jointed rock mass behaviour and failure mechanisms. International Journal of Rock Mechanics and Mining Sciences 140: 104700. https://doi.org/10.1016/j.ijrmms.2021.104700.

Maynard JB, Klein C (1995) Sedimentary and tectonic evolution of the Witwatersrand Basin. Geological Society of America Bulletin 107(6): 689–701.

Masethe, R. T., Durrheim, R. J., & Manzi, M. S. D. (2019). The seismic response to mining during the extraction of the Thuthukani shaft pillar, Kloof Operations, South Africa. In *Deep Mining 2019: Proceedings of the Ninth International Conference on Deep and High Stress Mining* (pp. 71-86). The Southern African Institute of Mining and Metallurgy.

Masethe, R. T., & Zvarivadza, T. (2025). The Impact of Scattered Mining on Gold Recovery: A Case Study in the Deep Level Gold Mine, South Africa. In *ARMA US Rock Mechanics/Geomechanics Symposium* (p. D021S002R003). ARMA.

McCarthy TS (2006) The Witwatersrand Supergroup. In: Johnson MR et al. (eds) The Geology of South Africa. Geological Society of South Africa, Johannesburg.

McCarthy TS, Stanistreet IG, Robb LJ (1990) Provenance and depositional environment of the Central Rand Group. South African Journal of Geology 93(2): 223–236.

Potvin Y, Hadjigeorgiou J, Stacey TR (2019) Ground support in mining and underground construction. CRC Press, Boca Raton.

Pretorius DA (1976) Gold distribution in the Central Rand Group. Economic Geology 71(6): 1087–1108.

Pretorius DA (1979) The depositional environment of the Witwatersrand Supergroup. Economic Geology 74(3): 460–476.

Qie L, Zhao J, Li X (2023) Failure mechanisms in fractured rock masses. Rock Mechanics and Rock Engineering 56(4): 2101–2115.

Robb LJ, Meyer FM (1995) The Witwatersrand Basin, South Africa: geological framework and mineralization processes. Ore Geology Reviews 10(1–2): 67–94.

Ryder JA, Jager AJ (2002) A textbook on rock mechanics for tabular hard rock mines. Safety in Mines Research Advisory Committee, Johannesburg.

SACS (1980) Stratigraphy of South Africa Part 1: Lithostratigraphy of the Republic of South Africa. Geological Survey of South Africa, Pretoria.

Sanders JV, Robb LJ, Groves DI (1994) Gold-bearing conglomerates of the Witwatersrand Basin. Economic Geology 89(3): 507–526.

Stacey TR (1989) Rock engineering design in deep-level gold mines. Journal of the South African Institute of Mining and Metallurgy 89(6): 183–195.

Tainton KM, Meyer FM (1990) Stratigraphy of the West Rand Group. South African Journal of Geology 93(3): 300–312.

Tucker RF, Viljoen RP, Anhaeusser CR (2016) Sedimentation and tectonic evolution of the Witwatersrand Basin. South African Journal of Geology 119(1): 1–16.

Viljoen RP (2009) An introduction to the Witwatersrand Basin geology. South African Journal of Geology 112(3–4): 211–230.

Viljoen RP, Viljoen MJ, Pearton TN (2016) The South Reef and its correlation across the Witwatersrand Basin. South African Journal of Geology 119(2): 345–360.

Wagner H, Schumann EH (1991) Rockburst control in South African gold mines. Journal of the South African Institute of Mining and Metallurgy 91(7): 209–217.

Wienand, G., Masethe, R. T., &Mgiba, C. (2024). High horizontal stress at depth incorporating reverse faults in Ya Rona Shaft, South Africa. In *New Challenges in Rock Mechanics and Rock Engineering* (pp. 965-970). CRC Press.

Zhou H, Zhang C, Li S (2023). Fault influence on underground excavation stability. Engineering Geology 310: 106900. https://doi.org/10.1016/j.enggeo.2022.106900